ACKNOWLEDGMENT

This paper is based on a research study conducted at the Pennsylvania Transportation Institute, Pennsylvania State University, under partial sponsorship of the Pennsylvania Department of Transportation. A full discussion of the study may be found in the final report for the project.

REFERENCES

1. J.R. Ingram. The Effects of Road Roughness on the Friction of a Slipping Tire. M.S. thesis. The Pennsylvania State University, University Park, 1972.
2. B.E. Quinn and S.E. Hildebrand. Effect of Road Roughness on Vehicle Steering. Highway Research Record 471, HRB, National Research Council, Washington, D.C., 1973, pp. 62-75.
3. F.J. Benvin. The Redesign of a Circular Track Apparatus for Traction Testing with Steering and Braking. Master of Engineering Paper. The Pennsylvania State University, University Park, 1976.
4. K.T. Cheng. Instrumentation and Data Processing System for Dynamic Tire Force Measurement. Report in Mechanical Engineering. The Pennsylvania State University, University Park, 1980.

Abridgment

Effect of Vehicle and Driver Characteristics on the Psychological Evaluation of Road Roughness

M. S. JANOFF and J. B. NICK

ABSTRACT

The objective of this paper is to summarize the results of an experiment that evaluated the effects of vehicle size, vehicle speed, residence of rating panel, and training of rating panel on the subjective evaluation of road roughness. The results of the panel ratings indicated that there was no significant effect of the different vehicle sizes or vehicle speeds used on the subjective evaluation of road roughness, and that trained raters (i.e., experts) evaluated roads the same as untrained raters (i.e., laymen). A small but significant effect of panel residence was found.

All panel ratings used the Weaver/AASHO scale employed in previous research (1). Five panels of 21 licensed drivers each--four of Pennsylvania residents and one of Florida residents--were used to obtain the subjective ratings.

Two groups of bituminous test sections--34 in Pennsylvania and 31 in Florida--that span a wide range of roughness were selected for the study. Table 1 summarizes the experimental plan and Table 2 provides an overview of the key variables and the hypotheses that were tested. The test sections spanned a range of roughness from 28 to 639 in. per mile.

EXPERIMENTAL PROTOCOL AND DATA COLLECTION

All test sections were selected, marked, and formed into two routes--one in Pennsylvania and one in Florida. Each section was then measured with a Mays Ride Meter.

Panel members, in groups of three or six, were given detailed instructions on how to rate and then were driven over the route to individually rate each section's ride quality. Mean panel ratings were computed from the individual ratings for each test section for each panel.

TABLE 1 Summary of Experimental Plan

Rating Scale	Weaver/AASHO
Panel	63 Pennsylvania-licensed drivers (3 groups of 21 each) 21 Florida-licensed drivers 21 Florida experts
Sites	34 in Pennsylvania 31 in Florida
Vehicles	2 Pennsylvania K-cars 2 Florida K-cars 1 Pennsylvania subcompact car
Vehicle speeds	One per site equal to the operating speed of the site (except for a subset used in the vehicle speed experiment)
Panel instructions	Given uniformly to all subjects

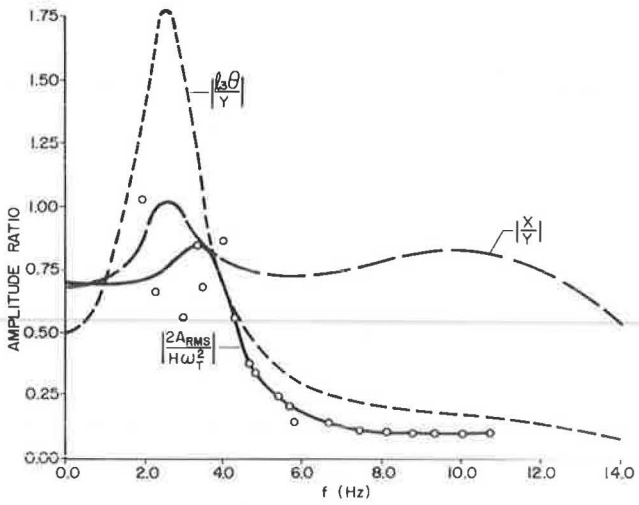

FIGURE 11 Normalized rms acceleration versus frequency for H = 0.5 in.

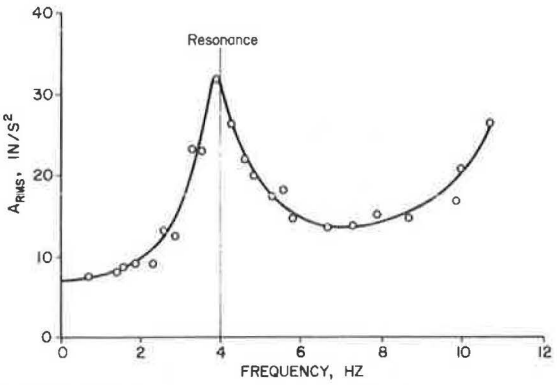

FIGURE 12 Rms acceleration versus frequency for H = 0.5 in.

CONCLUSIONS

Although it was expected that tire traction is reduced at higher frequencies (i.e., higher vehicle speeds or shorter wavelength), the loss was not expected to be as much as 30 percent at 11 Hz (a wavelength of 7.3 ft at 55 mph) for a track height of 0.5 in., peak-to-peak. Second, the traction loss was larger for the higher amplitude track. This would appear to be a logical trend, although more than two track heights would be necessary to obtain an exact relationship.

It was found that the average coefficient of friction was independent of the phases of the various components. Because all the factors are simply ratios of first order functions, this also appears to be a reasonable result. The minimum coefficient of friction is lower than μ_{avg} by a constant offset, independent of frequency. Under special conditions, such as stability during steering, this minimum value may be critical. As long as the braking duration covers several wavelengths, the average coefficient of friction will most likely dominate. This is in agreement with past work (1,2).

The rms acceleration data match the theoretical model fairly well except for the magnitudes at resonance. The reason for this is most likely the low value of damping used to obtain the theoretical resonances. In terms of the model of the present system, the only improvement might be to obtain the actual value of the damping coefficient and verify the inertias and spring constants. This should allow a better matching between the theoretical and experimental values of resonances and the magnitudes at these points.

For the system itself, an improvement should be made with respect to the pneumatic cylinders. They add the proper static loading to the system but, under dynamic conditions, they act as a spring when they should act as an inertia. This moves the first natural frequency up from the desired 1- to 2-Hz range into the 4-Hz range. A possible solution would be to replace the cylinders with lead weights hung on the test frame arm, as calculated by Benvin (3).

Further work will be conducted using a 1980 Pontiac Phoenix suspension system. Its lighter frame and MacPherson strut suspension should produce results that will be relevant for today's down-sized cars. Also, a roughness facility under construction at PTI will allow full-scale vehicle tests to further the research into traction loss due to roughness. Also, a special report by Task Group 1 of TRB Committee on Surface Properties-Vehicle Interaction is being prepared on The Influences of Roadway Surface Discontinuities on Safety. This report will also add to the knowledge of traction loss (safety) as affected by road roughness.

LIST OF SYMBOLS

A	The combined cross-sectional area of the pneumatic cylinders.
C_s	The linear viscous damping coefficient of the shock absorber.
F	The horizontal friction force between the tire and the track surface due to braking.
f_i	The ith natural frequency in hertz.
H	The peak-to-peak amplitude of the test track in inches.
I_o	Mass moment of inertia of the test frame.
K_p	Linear spring coefficient for the pneumatic cylinders.
K_s	Linear spring coefficient for the torsion bar.
K_t	Linear spring coefficient for the test tire.
ℓ_i	The ith lever arm dimension in inches.
m_F	The mass of the Toronado frame.
m_T	The mass of the wheel assembly.
N	The normal load at the test tire.
P_o	The spring force of the pneumatic cylinders.
R	The radius of the test tire.
T	The torque on the test tire due to braking.
TS	The absolute tangential velocity of the test frame.
u	Vertical displacement of the test frame at the point above the wheel assembly, ℓ = 66 inches.
V_o	The combined volume of the pneumatic cylinders.
W_i	The weight of the test frame.
W_F	The weight of the Toronado frame.
W_T	The weight of the wheel assembly.
W_S	The absolute tangential velocity of the test frame based on the test wheel.
X	Vertical displacement of the wheel assembly.
Y	Vertical displacement of the test track.
Z	Vertical displacement of the test frame at the point where the accelerometer is mounted, ℓ = 22 in.
λ	Wavelength of the test track, in inches.
μ	The kinematic coefficient of friction between the automobile tire and the test track.
θ	The rotational displacement of the test frame in radians.
ζ	The damping ratio for the system.

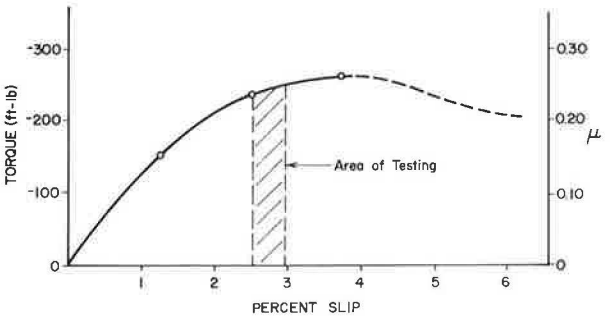

FIGURE 6 Tire traction versus percent slip.

shows that the rigorously precise $\mu(t)_{avg}$, which retains the phases in torque and normal load until the final step in the calculations, is only 0.29 percent less than μ_{avg}. Any phase shifts between the torque and the normal load are averaged out by the use of μ_{avg}. Therefore, in the following calculations μ_{avg} will be used.

It was found that the minimum coefficient of friction, μ_{min}, was offset from μ_{avg} by a constant increment, $\Delta\mu = 0.04375$ (see Figure 7). Because the normal load, N_{avg}, is an essentially constant 1,200 lb, the relationships between torque and frequency, and μ_{avg} and frequency, are identical. The two curves shown in Figures 8 and 9 indicate the relationships of both torque and coefficient of friction with increasing track frequency for both track amplitudes used. Both curves decay in an exponential manner. Figure 10 gives a combination and normalization of these curves to show the effect of track amplitude on the coefficient of friction. The data indicate that the higher amplitude track produces a greater loss of traction over the entire frequency range.

In Figure 11, the solid curve is the root mean square (rms) acceleration of the frame at a point directly above the test wheel, normalized by the input frequency of the track, $(H/2)w^2d$, and plotted against the frequency for H = 0.5 in. The dotted and dashed curves are the theoretical normalized rms accelerations for the test frame and the wheel assembly, respectively. Figure 12 gives the absolute plot of the rms acceleration versus frequency for the test frame where the accelerometer is mounted, at ℓ = 22 in. Scatter in the data at low frequency makes it difficult to draw a smooth curve through the data (Figure 11). However, Figure 12 shows that a smooth curve does indeed exist.

From visual observations during the operation of the system, it appears that the fundamental resonant frequency of the quarter-car model is about 4 Hz, and the tire assembly experiences resonance at about 11 to 12 Hz. The experimental plot in Figure 12 appears to verify both of these observations. The experimental plot in Figure 11 agrees fairly well with the theoretical curve. The only error is for the magnitude at resonance, and the primary reason for this is probably the low value of theoretical damping used.

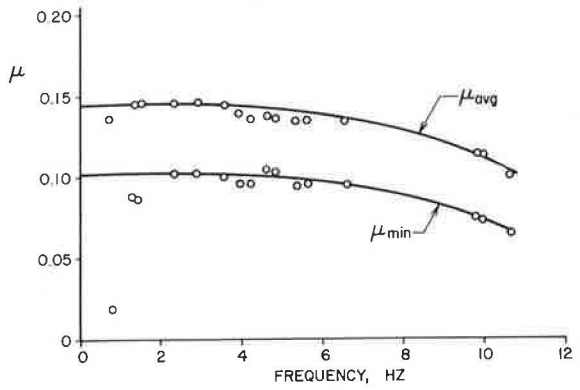

FIGURE 7 Variation in μ versus frequency.

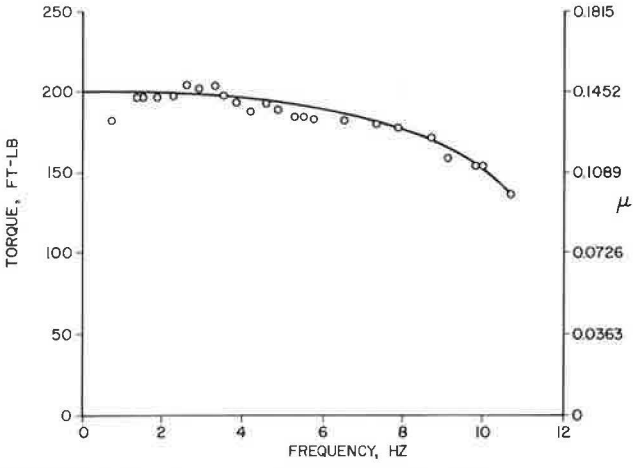

FIGURE 9 Traction versus frequency for H = 0.5 in.

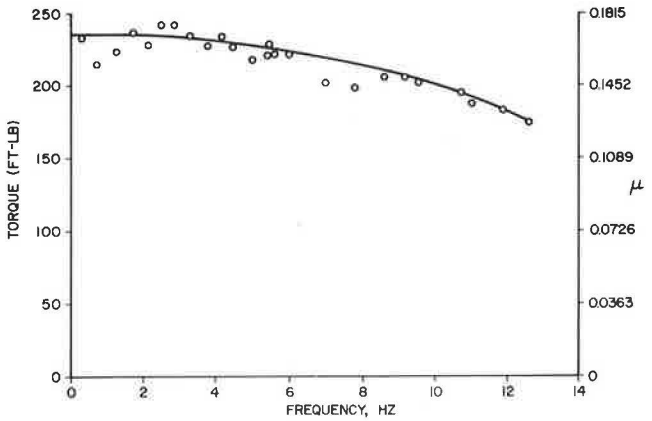

FIGURE 8 Traction versus frequency for H = 0.25 in.

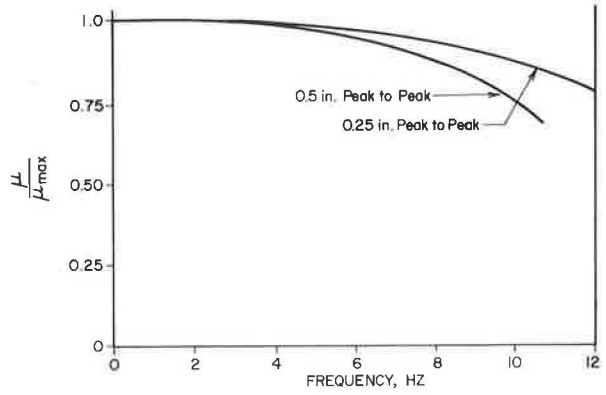

FIGURE 10 Traction versus frequency for both amplitudes.

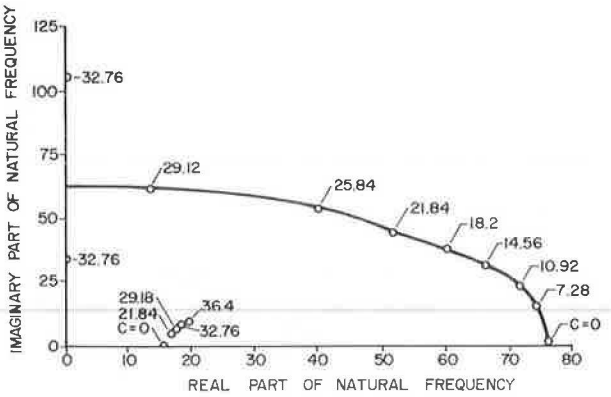

FIGURE 4 Natural frequencies versus damping factor.

cided to choose the highest value of C_s that still allows the resonances to approximately match the experimental resonances. This value is C_s = 14.56 lb-sec/in., and the corresponding natural frequencies and damping ratios are:

f_1 = 2.48 Hz and ξ_1 = 0.309, and
f_2 = 10.65 Hz and ξ_2 = 0.382.

The time-varying component of the normal load may be calculated as:

$$N(t)_T = K_E(Y - u) \tag{7}$$

where K_E is the equivalent spring coefficient for the system. It was experimentally measured to be 320 lb/m.

From the accelerometer mounted at ℓ_2, $\ddot{Z}$ is obtained. For small values of θ, the following approximations can be made:

$$\ddot{Z} = \ell_2\ddot{\theta} \tag{8}$$
$$\ddot{U} = \ell_3\ddot{\theta} \tag{9}$$

For $Y(t) = H/2 \sin(W_d t)$ the system is driven at the frequency W_d so that:

$$U = (-\ddot{U}_2/W_d) \tag{10}$$

therefore,

$$N(t)_T = K_E\,[Y(t) + (\ell_3/\ell_2)/(\ddot{Z}/W_d^2)] \tag{11}$$

and the total normal load becomes:

$$N(t) = N_0 + N(t)_T \tag{12}$$

It is essential to maintain the relative phases of Z and Y(t) during the recording of these values, otherwise the normal load, N(t), would be meaningless. As in the steady state case, the time-varying braking force, F(t), may be calculated as:

$$F(t) = T(t)/R \tag{13}$$

The time-varying coefficient of friction, $\mu(t)$, may then be calculated as:

$$\mu(t) = F(t)/N(t) \tag{14}$$

TESTING

Data were collected for two different amplitudes of track over the frequency range from 1 to 12 Hz. Figure 5 shows the instrumentation used to monitor the system and collect data.

The track speed tachometer was used to obtain the desired track frequency. The wheel speed tachometer was used to set the wheel braking slip with reference to the track speed by the following equation:

$$\%\,\text{slip} = [(TS - WS)/TS] \times 100 \tag{15}$$

The desired loading on the pneumatic cylinders was set by a pressure regulator. The lap reference counter has a microswitch that sent a signal every time the test frame passed a certain point on the track. The accelerometer measures the vertical acceleration, $\ddot{Z}$, of the test frame. The microswitch signal allows the relative phase of the accelerometer signal and the track amplitude to be determined. This is essential if the dynamic normal load, N(t), is to be calculated correctly using Equation 11. Finally, the torquemeter measures the torque at the test wheel for use in Equation 13.

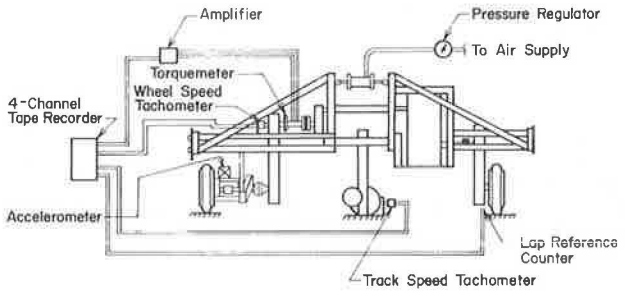

FIGURE 5 Instrumentation for data acquisition.

The torque, acceleration, lap counter, and track speed signals are continuously recorded by a four-channel tape recorder. The wheel speed only has to be measured once each time the percent slip is set, which is only when a new set of concrete slabs is put in place. Therefore, a special data set is taken at the start of each new track set, with the wheel speed replacing the lap counter signal.

The data were recorded and then digitized using an EAI 680 analog computer interfaced with a PDP DEC 10 digital computer. The data were then processed using the calibration curves to convert the signals into meaningful units of force, velocity, and acceleration.

RESULTS

In this section the physical results and the trends in the data recorded on the system are discussed. The variation in the coefficient of friction for changes in the braking slip is shown in Figure 6. The solid curve represents actual data recorded for this project. The dotted curve is the theoretical extrapolation to higher slip values based on Benvin's data (3). The maximum traction possible occurs at approximately 4 percent slip. The tests were run at between 2.5 and 3.0 percent slip.

Consider the relationship between $\mu(t)_{avg}$ and μ_{avg}. Comparison of the results for

$$\mu(t)_{avg} = [T(t)/R \times N(t)]\ \text{avg}$$

versus

$$\mu_{avg} = T_{avg}/(R \times N_{avg})$$

be considered. The circular track is equipped with pressure cylinders that can apply additional loading to the Toronado suspension. The pressure cylinders, along with the natural weight and inertia of the test arm frame, supply a known normal load, N, at the wheel equal to that of the front right quarter of a Toronado under both static and dynamic conditions.

The circular track test frame is equipped with a variable ratio gear train which, when adjusted from equilibrium, applies a braking slip between the drive wheel and the test wheel. This creates a braking torque, T, on the test wheel, which can be measured using an in-line torquemeter. Under steady state operating conditions, with a given percent slip and cylinder loading and with the flat track in place, the horizontal braking force, F, between the tire and the track surface is

$$F = T/R \tag{1}$$

[Note: For explanations of the variables used in the equations, please refer to the List of Symbols at the end of this paper.]

The coefficient of friction, μ, between the tire and the track surface is:

$$\mu = F/N \tag{2}$$

When a sinusoidal track surface is used, the values of torque and normal load will vary sinusoidally about a constant value. A simple procedure would be to assume that, over several revolutions of the system at steady state, the average values of F and N will equal their constant values. Therefore, these average values, F_{avg} and N_{avg}, could be measured and used to calculate the coefficient of friction, μ. However, a more rigorous procedure was chosen which stores both the constant values and the variations in magnitude and phase in the values of torque and normal load. Throughout the calculations of the coefficient of friction, an average value of μ may be the same as that calculated by the simpler procedure; but it is possible that the dynamics of the system, especially at resonance, could result in phase shifts in the relative peaks of F and N, which would affect the instantaneous, and possibly even the average, values of μ. This procedure yields the average value of μ as well as the instantaneous maximum and minimum values. These values may turn out to be as important as the average value.

To perform this procedure, the vertical acceleration of the frame was measured to determine the changes in the normal load, N(t), due to inertial loadings. The time-varying torque, T(θ), was recorded by the torquemeter just as for the steady state case.

To calculate the time-varying normal load, N(t), from the acceleration data, the dynamics of the system must be considered. The free-body diagram in Figure 3 represents the test arm, with the Toronado suspension reduced to a 2-degrees-of-freedom system.

The summing of moments about 0 for the static case yields

$$\Sigma M_0 = P_0\ell_3 + W_1\ell_1 + W_F\ell_3 = N_0\ell_3 \qquad (N_0 = 1{,}257 \text{ lb}) \tag{3}$$

This is the steady state value of the normal load.

The summing of moments about point 0 for the dynamic case yields the differential equations of motion for the system:

$$(I_o + m_F\ell_3^2)\ddot{\theta} + C_S\ell_3^2\dot{\theta} + (K_S\ell_3^2 + K_p\ell_4^2)\theta = K_S\ell_3 x + C_S\ell_3\dot{x} \tag{4}$$

$$m_T\ddot{x} + C_S\dot{x} + (K_T + K_S)x = K_S\ell_3\theta + K_T Y + C\ell_3\dot{\theta} \tag{5}$$

The equations were solved using the mode superposition method. Assuming the general solutions:

$$x(t) = \bar{x}e^{jwt}$$
$$\theta(t) = \theta e^{jwt}$$

where w is complex, and substituting all known values into Equations 4 and 5, the resulting characteristic equation is obtained:

$$1{,}379{,}028.8 - (6{,}103.8 - 8.79 \times 10^{-4}C_S^2)\,w^2 + w^4 + j(3{,}375.4\,C_S w - 4.739\,C_S w^3 \tag{6}$$

The roots of this equation are obtained by setting it equal to zero. The roots are the natural frequencies for the system. Because the damping term, C_S, is difficult to determine accurately, a computer program was written to solve Equation 6 for a range of values of C_S between 0 and 36.4 lb-sec/in. Figure 4 shows the resulting root locus plot.

A typical damping ratio for a quarter-car would be on the order of $\xi = 0.8 - 1.0$. This would correspond to a value of C_S between 37.7 and 47.1 lb-sec/in. A value this high produces meaningless roots for the system. Thus, for the analysis, it was de-

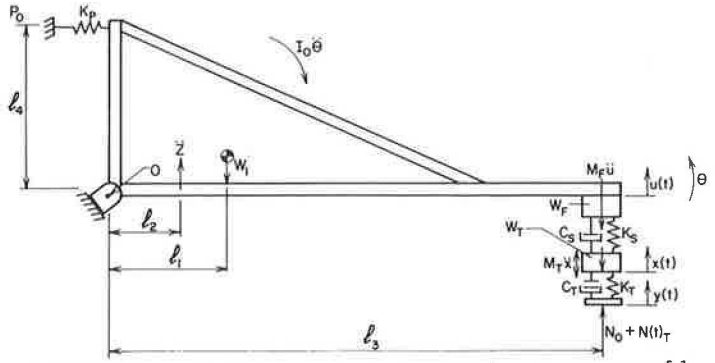

FIGURE 3 Free body diagram for the test frame and wheel assembly.